The Journal of Arthroplasty xxx (2020) 1–8

Contents lists available at ScienceDirect

The Journal of Arthroplasty

journal homepage: www.arthroplastyjournal.org

Bone Mineral Density and Cortical-Bone Thickness of the Distal Radius Predict Femoral Stem Subsidence in Postmenopausal Women

Sanaz Nazari-Farsani, MSc, Mia E. Vuopio, MSc, Hannu T. Aro, MD, PhD *

Department of Orthopaedic Surgery and Traumatology, Turku University Hospital and University of Turku, Turku, Finland

ARTICLE INFO

Article history:
Received 18 January 2020
Received in revised form
21 February 2020
Accepted 26 February 2020
Available online xxx

Keywords:
cementless total hip arthroplasty
radiostereometric analysis (RSA)
osteoporosis
cortical bone
DXA
pulse-echo ultrasonometry

ABSTRACT

Background: The distal radius is an optional site for evaluation of bone quality in postmenopausal women before cementless total hip arthroplasty. We hypothesized that dual-energy X-ray absorptiometry (DXA) and pulse-echo ultrasonometry of the distal radius may help discriminate subjects at high risk of femoral stem subsidence.

Methods: A prospective cohort of postmenopausal women with primary hip osteoarthritis underwent total hip arthroplasty with implantation of a parallel-sided femoral stem. Postoperative stem migration was measured using radiostereometric analysis. Preoperatively, subjects had multisite DXA measurement of bone mineral density (BMD) and pulse-echo ultrasonometry of the cortical-bone thickness. The diagnostic abilities of these methods to discriminate <2 mm and ≥2 mm femoral stem subsidence were tested.

Results: The accuracy of the distal radius BMD and cortical-bone thickness of the distal radius were moderate (area under the curve, 0.737 and 0.726, respectively) in discriminating between <2 mm and ≥2 mm stem subsidence. Women with low cortical-bone thickness of the radius were more likely (odds ratio = 6.7; P = .002) to develop stem subsidence ≥2 mm. These subjects had lower total hip BMD (P = .007) and reduced thickness of the medial cortex of the proximal femur (P = .048) with lower middle (P < .001) and distal (P = .004) stem-to-canal fill ratios.

Conclusion: Femoral stem stability and resistance to subsidence are sensitive to adequate bone stock and unaltered anatomy. DXA and pulse-echo ultrasonometry of the distal radius may help discriminate postmenopausal women at high risk of stem subsidence.

In total hip arthroplasty (THA), uncemented femoral stems rely on the initial press-fit fixation against the cortical bone [1]. In postmenopausal women, endosteal trabeculation and increased intracortical porosity [2] pose natural difficulties in achieving axial and rotational stem stability. Women with a low systemic bone mineral density (BMD) have shown to have limited migration of an anatomically designed femoral stem [3] and a double-wedged straight femoral stem [4] during the first months after surgery before osseointegration.

A parallel-sided femoral stem was designed to engage the metaphyseal cortical bone in the medial-lateral plane only [5,6]. The use of the stem requires adequate bone stock and unaltered femoral geometry [7], but no exact definitions have been determined for these requirements. In radiostereometric analysis (RSA), the stem allowed subsidence of 1.5 mm (95% confidence interval [CI], 0.1-2.9 mm) even in women with normal hip BMD and Dorr type A or B femur anatomy [8]. Although this migration was not detrimental to osseointegration, it demonstrates challenges in obtaining secure press-fit fixation in postmenopausal women and difficulties in finding appropriate criteria for adequate bone stock and proximal femur anatomy.

Dual-energy X-ray absorptiometry (DXA) may give a misleading impression of hip BMD in patients with hip osteoarthritis. Women with moderate to severe radiographic hip osteoarthritis have a 9%-10% higher femoral neck BMD compared to that in those without osteoarthritis [9]. The distal radius is an optional site for

One or more of the authors of this paper have disclosed potential or pertinent conflicts of interest, which may include receipt of payment, either direct or indirect, institutional support, or association with an entity in the biomedical field which may be perceived to have potential conflict of interest with this work. For full disclosure statements refer to https://doi.org/10.1016/j.arth.2020.02.062.

* Reprint requests: Hannu T. Aro, MD, PhD, Turku University Hospital TE-1, Room E115 PL 52, FI-20521, Turku, Finland.

https://doi.org/10.1016/j.arth.2020.02.062

DXA evaluation of systemic BMD in patients with hip osteoarthritis [10].

Pulse-echo ultrasonometry for determining cortical-bone thickness of the proximal tibia, combined with patient characteristic data (age, weight, and height) in a density index, is approved by the Food and Drug Administration as a portable prescreening test for hip osteoporosis, reducing the need for DXA [11]. The original approach included the measurement of cortical-bone thickness at 3 sites (distal radius, proximal tibia, and distal tibia) and the calculation of a multisite density index, which showed a correlation with the proximal femur BMD [12].

The purpose of this study is to evaluate the diagnostic ability of the distal radius DXA and pulse-echo ultrasonometry in the prediction of stem subsidence. We hypothesized that these methods may help discriminate postmenopausal women who are prone to stem subsidence after cementless THA.

Patients and Methods

Study Design

This study focused on a trial cohort of postmenopausal women (Clinicaltrials.gov NCT01926158) who had a preoperative multisite DXA before cementless THA and underwent successful postoperative RSA of femoral stem migration. The subjects were participants of a single-center, double-blinded, placebo-controlled, randomized clinical trial [8] approved by the Ethics Committee of the Hospital District of South-West Finland (decisions 105/2012 and 484/2017) and Finnish Medicines Agency (decision 183/06.00.00/2012, EudraCT 2011-000628-14). All participants provided written informed consent before enrollment. The trial examined the effects of antiresorptive denosumab in physically active postmenopausal women who would likely benefit from the long-term endurance of cementless THA. Denosumab has a strong influence on cortical bone remodeling of the proximal femur in postmenopausal women [13]. It was expected to have a dual effect by preventing periprosthetic bone resorption (primary end point), and thereby reducing the amount of initial femoral stem migration occurring before osseointegration (secondary end point).

Based on an amendment approved by the ethics committee, the subjects underwent preoperative multisite pulse-echo ultrasonometry of cortical-bone thickness as an off-trial examination (Fig. 1). The diagnostic accuracy of the distal radius BMD measured by DXA and the cortical-bone thickness of the distal radius measured by pulse-echo ultrasonometry were tested for discrimination between femoral stem subsidence of <2 mm and ≥2 mm at 48 weeks. Two reference parameters, namely total hip BMD (measured by DXA) and the density index (measured by pulse-echo ultrasonometry), were also tested. A stem subsidence threshold of 2 mm was adopted from the literature [14].

Patients and Screening Studies

The inclusion criteria included patients aged between 60 and 85 years with a diagnosis of primary osteoarthritis of the hip. The exclusion criteria included Dorr type C femur morphology, previous

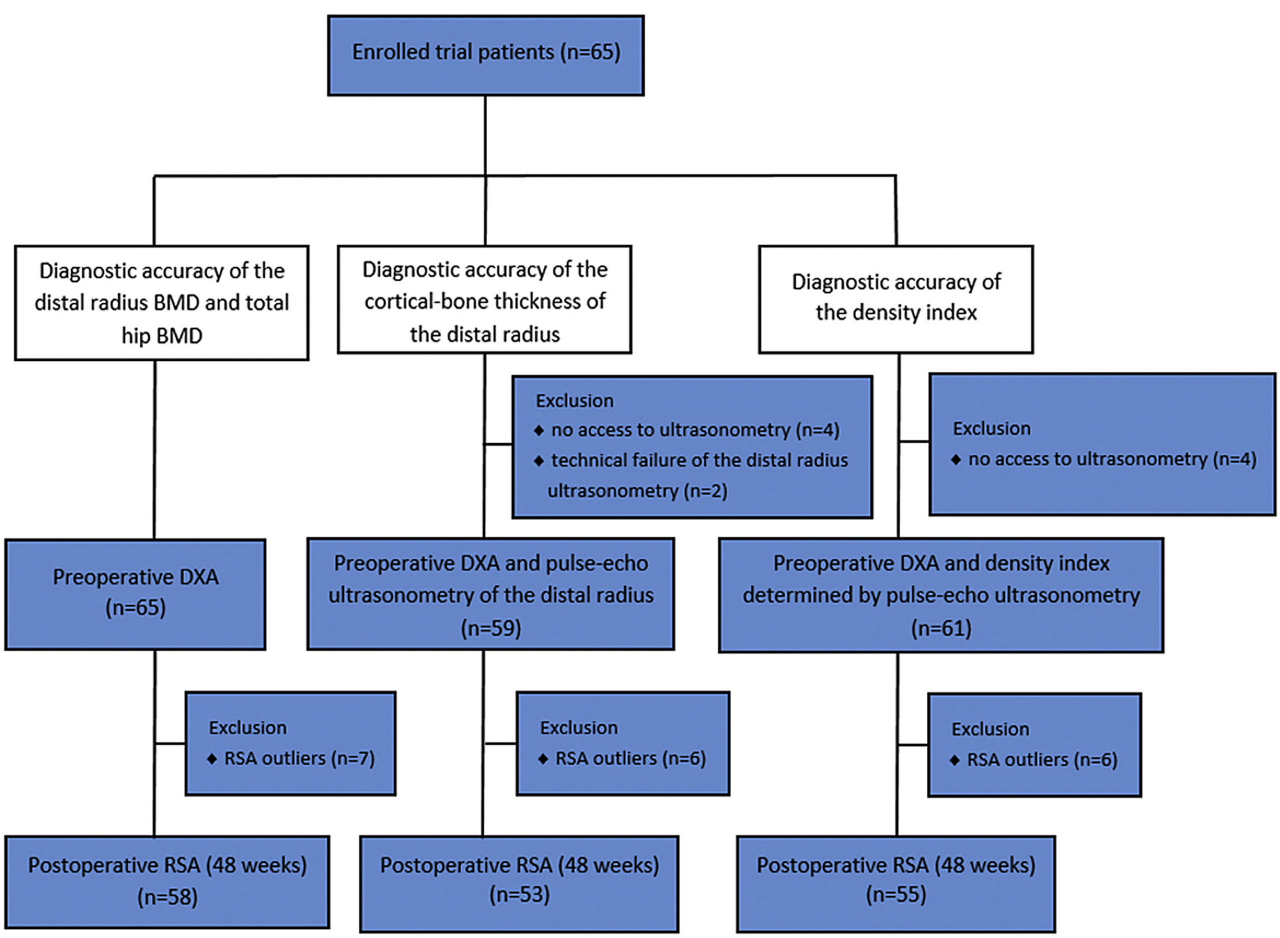

Fig. 1. Study flow diagram. BMD, bone mineral density; DXA, dual-energy X-ray absorptiometry; RSA, radiostereometric analysis.

surgery of the index hip, severe osteoporosis (hip or lumbar spine T-score < −4.0), evidence of secondary osteoporosis, use of osteoporosis drugs or other prescription drugs affecting bone metabolism, rheumatoid arthritis or any other inflammatory arthritis, or any condition that may affect the ability to perform the functional assessments required by the protocol.

Screening included DXA (Hologic, Discovery A; Hologic Inc, Marlborough, MA) of the proximal femurs (the operated hip only in subjects with previous THA of the contralateral hip), lumbar spine, and distal (one-third) radius of the nondominant hand. According to the criteria of the International Society for Clinical Densitometry, the measurement of the distal radius BMD was not included in the diagnosis of osteoporosis or osteopenia. Serum levels of ionized calcium and 25-hydroxyvitamin D were measured for exclusion of hypocalcemia and vitamin D deficiency, respectively.

Pulse-Echo Ultrasonometry

Preoperative pulse-echo ultrasonometry of cortical-bone thickness was performed using a mobile device (Bindex, Bone Index Finland Ltd, Kuopio, Finland) [11,12]. Of the 65 eligible participants, 4 did not undergo ultrasound prescreening due to the unavailability of the device at the start of the screening process (Fig. 1). According to the recommended technique [11,12], the measurements were conducted on predetermined sites, localized using distance measurements from the anatomic landmarks (the distal radius at one-third of the distance from the radial styloid process to the proximal radial head, and the proximal and distal tibia at one-third and two-thirds of the distance from the knee joint space to the medial malleolus, respectively). Measurements were performed by 2 study physiotherapists. The examiners had no information on DXA results. Five successful repeated measurements in each location were taken and averaged. After completion of the measurement protocol for each subject, the device calculated the density index (g/cm^2) based on the thickness measurements and patient characteristics (age, weight, and height). Due to technical problems, the density index was calculated based on a single-site measurement of the proximal tibia in 2 subjects. The intraobserver and interobserver variations, presented as coefficient of variation (CV) for the measurement of density index, were analyzed using triplicate measurements of the 3 anatomic locations in an uninterrupted sequence in 45 patients. The test-retest variability was 4.3% (95% CI, 3.5-5.1) for the triplicate measurements, and CVs of the 2 examiners were 3.9% and 4.7%.

Surgery and Trial Intervention

All patients underwent THA using a single-wedged, parallel-sided femoral stem (Accolade II, Stryker Orthopedics, Mahwah, NJ) with a 36-mm metallic head and a porous-coated uncemented acetabular cup with a polyethylene liner. Surgery was performed using an anterolateral Hardinge approach. The patients were mobilized using standard physiotherapy, and immediate unrestricted weight-bearing was encouraged with the aid of crutches. Patients were randomly assigned to receive antiresorptive denosumab treatment (a subcutaneous injection of 60 mg every 6 months) or placebo for 1 year, which started 4 weeks before surgery. As reported [8], the denosumab-treated subjects showed increased periprosthetic BMD in clinically relevant regions of the proximal femur, but the treatment response was not associated with any reduction in the initial stem migration. No major surgical complications (dislocations, periprosthetic fractures, or infection)

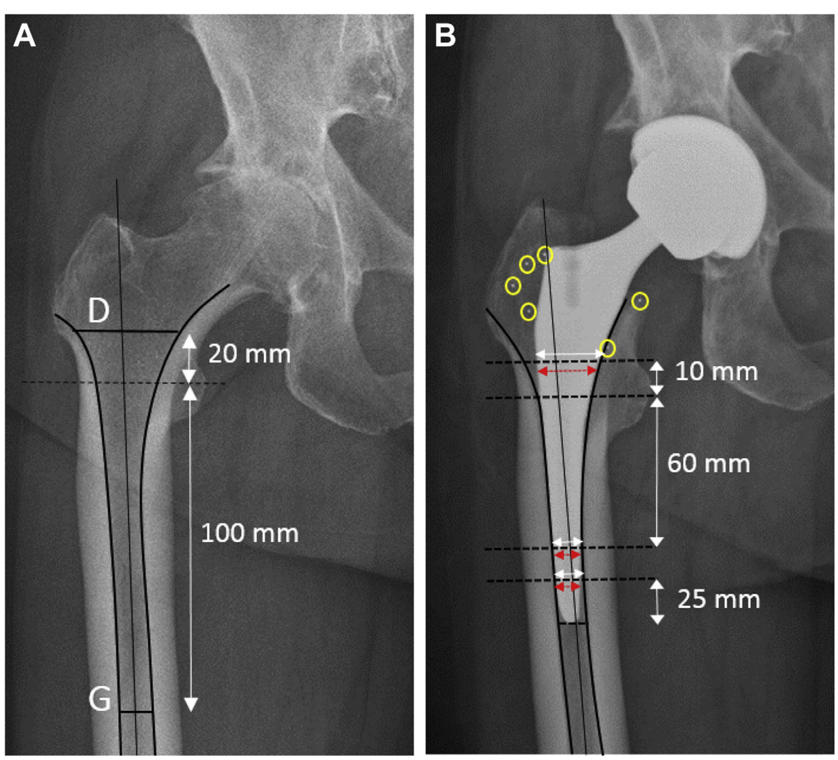

Fig. 2. Preoperative canal flare index is calculated as the ratio of D to G (A). The postoperative stem-to-canal fill ratio is measured as the stem width over the femoral canal width in 3 locations; 10 mm above the lesser trochanter (proximal), 60 mm below the lesser trochanter (middle), and 25 mm above the distal tip (distal) (B). At the proximal level, the measurement of the canal width does not take into account the lateral gap between the stem and the cortical bone. The implanted radiostereometric analysis bone markers are marked by yellow circles over the greater and lesser trochanters (B).

or drug-related adverse events were reported during the 1-year trial period and during a 3-year safety follow-up.

Radiostereometric Analysis

The accuracy and precision of the applied model-based RSA technique was verified in a phantom model before the trial [15]. RSA was performed according to the RSA guidelines [16,17]. The computer-aided design surface models of each stem size were converted to the model-based format by a third party (Biomechanics and Imaging Group, Leiden University Medical Center, Leiden, Netherlands). During surgery, multiple tantalum RSA markers were implanted into the trochanteric bone (Fig. 2). The stability and adequate distribution of bone markers were assessed by calculating the mean error of the rigid body fitting (upper limit ≤0.35) and the condition number (upper limit ≤150). RSA imaging was performed within 3 days after the surgery (baseline) and repeated after 12, 22, and 48 weeks. The time-related translations and rotations of the *x*-, *y*-, or *z*-axes were measured using MBRSA software (version 3.34; Medis Specials BV, Leiden, Netherlands) with combined stem-head models. The selected end points were translation along the *y*-axis (stem subsidence) and rotation around the *y*-axis (stem rotation) at 48 weeks, which represented the 2 principle directions of postoperative stem migration. As reported [8,15], the accuracy of the model-based RSA was 30 μm, and the clinical precision was 110 μm for the measurement of stem subsidence. For the measurement of stem rotation around the *y*-axis, the accuracy was 0.39°, and the clinical precision was 1.04°. Seven outliers with excessive stem subsidence and/or rotation around the *y*-axis were detected. The outliers were identified by the applied statistical software (IBM SPSS Statistics version 25.0), which defined the outliers as $Xi \geq Q3 + (1.5 \times$ interquartile range [IQR]) and $Xi \leq Q1 - (1.5 \times IQR)$, where Q1 and Q3 represent the first and third quartile limits, respectively, and the IQR represents the difference between Q1 and the Q3 limit. The analysis gave the following cutoff values for the outliers: stem subsidence >5.44 mm, and/or stem rotation >5.52° of internal rotation (retroversion), or >4.32° of external rotation. The outliers were not included in the current analysis. After exclusion of the outliers, the subsidence and rotation values showed a normal distribution (Shapiro-Wilk normality test). The analyzed cohort, without outliers (n = 58; Table 1), included 32 subjects with stem subsidence of <2 mm and 26 subjects with stem subsidence of ≥2 mm. There were missing RSA data from one subject at 22 weeks and 48 weeks. The subject exhibited a stem subsidence of 2.29 mm at 12 weeks and had an unremarkable clinical recovery and radiographic outcome. The subject's data were included and analyzed in the group with stem subsidence of ≥2 mm.

Radiographic Assessments

The canal flare index (CFI) [18] was measured from anteroposterior radiographs using computerized methods (Rhinoceros software, version 3.0SR5b, Robert McNeel & Associates, Seattle, WA). The CFI was calculated as the ratio of D to G, where D is the metaphyseal width, 20 mm proximal to the most prominent point of the lesser trochanter, and G is the width of the intramedullary femoral isthmus, 100 mm distal to the lesser trochanter (Fig. 2A). As described for the radiographic fit-and-fill analysis [5], the ratio of the stem width over the femoral canal width was measured 10 mm above the lesser trochanter (proximal stem), 60 mm below the lesser trochanter (middle stem), and 25 mm above the distal tip (distal stem; Fig. 2B). Exploratory end points included the radiographic assessment of stem osseointegration based on the criteria of Engh et al [19].

Table 1
Baseline Demographics and Clinical Characteristics in All Subjects and in Subjects With the Cortical-Bone Thickness of the Radius Above or Below the Cutoff Value.

Parameters	All Subjects	Radius Cortical-Bone Thickness ≥ 2.33 mm	Radius Cortical-Bone Thickness < 2.33 mm	*P* Value[a]
No. of cases	58	26	27	
Age, y	69 (60-84)	68 (61-79)	69 (60-78)	.58
BMI, kg/m^2 (SD)	28 (4.7)	29 (5.4)	27 (4.2)	.27
ASA classification, n				
Class 1	3	1	2	.44
Class 2	31	13	17	
Class 3	24	12	8	
Systemic BMD, n				
Normal bone (T-score ≥ −1.0)	30	18	10	.041
Osteopenia (−2.5 < T-score < −1.0)	26	8	15	
Osteoporosis (T-score ≤ −2.5)	2	0	2	
Total hip BMD, g/cm^2 (SD)	0.93 (0.14)	0.98 (0.15)	0.88 (0.12)	.007
Femoral neck BMD, g/cm^2 (SD)	0.84 (0.14)	0.91 (0.14)	0.78 (0.12)	.001
Lumbar spine BMD, g/cm^2 (SD)	1.01 (0.18)	1.09 (0.20)	0.93 (0.13)	.001
Distal radius BMD, g/cm^2 (SD)	0.66 (0.07)	0.70 (0.06)	0.62 (0.06)	<.001
Femur cortical thickness, mm (SD)	9.4 (1.5)	10.0 (1.3)	9.1 (1.5)	.034
Medial cortex	12.1 (2.8)	13.0 (2.9)	11.5 (2.5)	.048
Lateral cortex	6.8 (1.3)	6.9 (1.1)	6.6 (1.6)	.54
Canal flare index (SD)	3.8 (0.7)	4.0 (0.7)	3.7 (0.6)	.07
Stem-to-canal fill ratio				
Proximal stem (SD)	0.98 (0.02)	0.98 (0.02)	0.97 (0.03)	.27
Middle stem (SD)	0.86 (0.09)	0.91 (0.07)	0.82 (0.09)	<.001
Distal stem (SD)	0.85 (0.09)	0.89 (0.09)	0.82 (0.09)	.004
Stem size (SD)	3.2 (1.0)	3.0 (1.0)	3.4 (1.0)	.09
Denosumab				
Active drug	31	16	14	.48
Placebo	27	10	13	

BMI, body mass index; SD, standard deviation; ASA, American Society of Anesthesiologists.
[a] Comparison of subjects with the radius cortical-bone thickness of ≥2.3 mm or <2.3 mm with 2-tailed Student *t*-test or chi-square test.

Assessment of Functional Status and Physical Activity

As an objective measure of the functional status [20], a self-selected comfortable spontaneous walking speed (m/s) was measured using a portable, validated inertial, sensor-based gait analysis system (RehaGait; Hasomed GmbH, Magdeburg, Germany) [21]. The mean CV of the repeated measurements was 4.7%. Preoperative and postoperative assessments of daily walking activity were performed [22]. Daily accounts of accumulated walking steps using digital pedometers were recorded by each patient over 7-day periods that were typical or representative of their usual activity. The preoperative and repeated postoperative clinical assessments included recordings of standard patient-reported outcome measures, including the Harris hip score and the Western Ontario and McMaster Universities Osteoarthritis Index.

Statistical Analysis

The diagnostic accuracy of the distal radius BMD and the cortical-bone thickness of the distal radius and 2 reference parameters (density index and total hip BMD) was tested using receiver operating characteristic (ROC) curves. ROC curves were created by plotting the true-positive rate (sensitivity) against the false-positive rate (1—specificity; Fig. 3). Statistics included the estimated area under the curve (AUC) with 95% CIs. The data of ROC curves were used to determine cutoff values, corresponding to the maximum sum of sensitivity and specificity in discrimination between stem subsidence of <2 mm and ≥2 mm. A binary logistic regression analysis was conducted to evaluate the odds ratio, presented with 95% CIs, for developing stem subsidence of ≥2 mm with the cutoff value determined by the ROC curve analysis.

Subjects with a cortical-bone thickness of the radius equal to or above and below the ROC curve-driven cutoff value were compared for the magnitude of stem migration, baseline demographics, and clinical and radiographic outcomes with 2-tailed Student *t*-test for continuous variables and with chi-square test for categorical variables.

To confirm the relevance of the applied technique in multisite pulse-echo ultrasonometry measurements, density index values were plotted against the reference standard (DXA-measured total hip BMD) using Pearson linear correlation analysis. The distribution of subjects with a normal (total hip and/or femoral neck T-score ≥ -1.0) and low hip BMD (total hip and/or femoral neck T-score < -1.0) was analyzed within the quartiles of the density index using the chi-squared test.

$P < .05$ was considered statistically significant. Analyses were performed using IBM SPSS Statistics 25 software (International Business Machines Corp, Armonk, NY).

Results

Cortical-Bone Thickness of the Distal Radius and the Distal Radius BMD

The ROC curve analysis for the cortical-bone thickness of the radius measured by pulse-echo ultrasonometry (Fig. 3A) determined a cutoff value of 2.33 mm for discriminating between stem subsidence of <2 mm and ≥2 mm. The AUC value was 0.726 (95% CI, 0.584-0.867; $P = .005$). In the logistic regression analysis, subjects

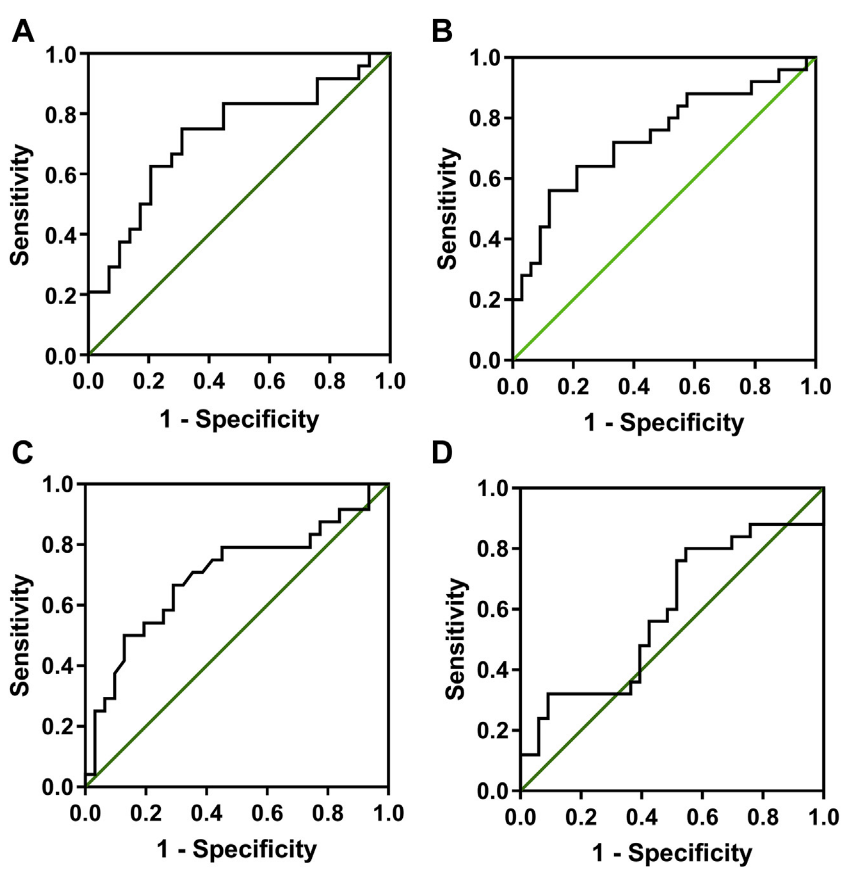

Fig. 3. Receiver operating characteristic curve analyses (black line) to determine the cutoff values of the cortical-bone thickness of the radius (A), distal radius bone mineral density (BMD) (B), density index (C), and total hip BMD (D) in discriminating between stem subsidence of <2 mm and ≥2 mm. The reference line is indicated in green.

with cortical-bone thickness of the radius below the cutoff value (<2.33 mm) were more likely (odds ratio = 6.7; 95% CI, 2.0-22.4) ($P = .002$) to develop stem subsidence of ≥2 mm than those with cortical-bone thickness above the cutoff value (≥2.33 mm).

As the standard reference, the distal radius BMD, measured by DXA, confirmed the results of pulse-echo ultrasonometry. ROC curve analysis for the distal radius BMD (Fig. 3B) determined a cutoff value of 0.668 g/cm^2 for discriminating between stem subsidence of <2 mm and ≥2 mm. The AUC value was 0.737 (95% CI, 0.603-0.871; $P = .002$).

At 48 weeks, the magnitude of stem subsidence was 1.31 mm (95% CI, 0.79-1.83) in subjects with a cortical-bone thickness of the radius greater than or equal to the cutoff value and 2.43 mm (95% CI, 1.83-3.03) in subjects with a cortical-bone thickness below the cutoff value (mean difference, 1.11 mm; 95% CI, 0.34-1.89; $P = .006$; Fig. 4A). No significant intergroup differences in stem rotation were found (Fig. 4B). Other axes showed no significant intergroup differences in stem translations and rotations (Supplementary Table 1).

The comparison of baseline demographics of subjects with a cortical-bone thickness of the radius greater than or equal to or below the cutoff value showed distinct differences (Table 1). Subjects with a cortical-bone thickness of the radius below the cutoff value had lower BMDs at all 3 sites. They also had a significantly reduced thickness of the medial cortex of the proximal femur and exhibited lower stem-to-canal fill ratios at the middle and distal femoral stem regions (Table 1). Despite the difference in stem subsidence, no significant intergroup differences were found in 48-week patient-reported outcome measures and functional outcomes (including walking speed and walking activity) and the 2-year radiographic stem osseointegration (Table 2).

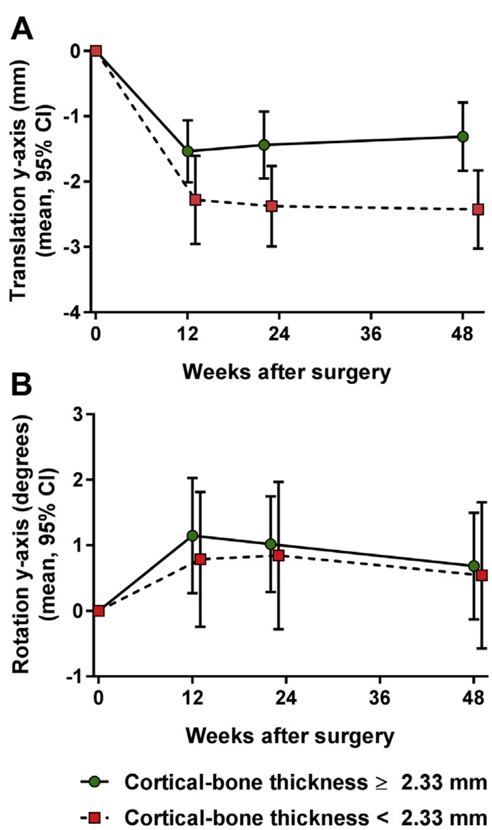

Fig. 4. The subsidence (A) and rotation (B) of the femoral stem, measured by model-based radiostereometric analysis, in subjects with the cortical-bone thickness of the radius above and below the cutoff value of 2.33 mm. The values are the means (95% confidence interval [CI]).

Density Index and Total Hip BMD

In the ROC analysis for the density index (Fig. 3C), the cutoff value was 0.903 g/cm^2, and the AUC value was 0.698 (95% CI, 0.552-0.845; $P = .012$). Total hip BMD (Fig. 3D) failed to discriminate between acceptable and unacceptable femoral stem subsidence. The AUC value was 0.588 (95% CI, 0.435-0.741; $P = .26$).

The density index showed a linear correlation ($r^2 = 0.306$, $P < .001$) with total hip BMD measured by DXA. The proportion of women with a normal or low hip BMD was different between the quartiles of the density index ($P < .001$). The highest quartile of the density index only had subjects with a normal hip BMD.

Discussion

The cortical-bone thickness of the distal radius measured by pulse-echo ultrasonometry, as well as the DXA-measured distal radius BMD, helped discriminate postmenopausal women at high risk of early stem subsidence. Women with a low cortical-bone thickness of the radius (less than the cutoff value of 2.33 mm) turned out to have cortical-bone thinning and reduced BMD also in the proximal femur. Probably due to these structural changes, the subjects were 6.7 times more likely to develop stem subsidence. They did not differ in age, body mass index (BMI), or walking speed; calling for the need of screening procedures, such as DXA or pulse-echo ultrasonometry of the distal radius, to recognize impaired bone quality before surgery. Importantly, the BMD of the operated hip determined by DXA failed to identify women prone to stem subsidence.

The parallel-sided femoral stem, like other stem designs [3,4], seems to subside to a certain extent before osseointegration in postmenopausal women with reduced bone mass. However, bone quality is only one of many potential confounding factors dictating the magnitude of stem subsidence. This probably explains why despite a high statistical significance, the cortical-bone thickness of the distal radius (like the distal radius BMD) attained only moderate accuracy (defined as AUC between 0.70 and 0.90) in distinguishing subjects at high risk of stem subsidence. Undoubtedly, the clinical prediction of stem subsidence with a high diagnostic accuracy (generally defined as AUC > 0.90) will be highly challenging.

The primary stability of the parallel-sided stem was predictable in postmenopausal women with a cortical-bone thickness of the radius above the cutoff value. In these subjects, stem-to-canal fill ratios corresponded to those reported in the literature [5], and stem subsidence was within the reported range of RSA-measured subsidence (from 0.7 mm to 1.7 mm) of different stems in male and female THA populations of different ages [23–25].

The proximal stem represents the main engagement site of the parallel-sided femoral stem against the calcar bone [6]. Although the subjects with low cortical-bone thickness of the radius showed a high stem-to-canal fill ratio of the proximal stem, their stems tended to subside. In these subjects, the lower stem-to-canal fill ratios, measured in the middle and distal stem sections, can be explained by the reduced thickness of the medial femoral cortex. Based on the original description [26], thinning of the medial cortex of the femur is a main feature of Dorr type B femurs. Patients also exhibited a tendency toward a lower CFI as a sign of a slightly enlarged medullary canal. However, it must be emphasized that all our enrolled subjects, except 4 marginal CFI outliers between 2.8 and 2.9, had a CFI within a normal range (CFI, 3.0-4.7) or had a champagne flute femur anatomy (CFI > 4.7). These emerging

Table 2
PROMs, Functional and Radiographic Outcome.

Parameters	All Subjects	Radius Cortical-Bone Thickness ≥ 2.33 mm	Radius Cortical-Bone Thickness < 2.33 mm	*P* Value[a]
WOMAC score (SD)				
Preoperative	48.2 (15.4)	48.0 (14.4)	46.6 (14.4)	.73
Postoperative 48 wk	16.5 (15.8)	16.1 (15.0)	16.7 (17.0)	.89
HHS (SD)				
Preoperative	47.9 (14.8)	48.2 (15.4)	47.8 (14.5)	.93
Postoperative 48 wk	79.9 (13.4)	78.9 (13.9)	82.6 (9.7)	.26
Walking speed, m/s (SD)				
Preoperative	0.89 (0.27)	0.90 (0.26)	0.90 (0.25)	.99
Postoperative 48 wk	1.16 (0.23)	1.16 (0.24)	1.12 (0.31)	.62
Walking activity, steps/d (SD)				
Preoperative	3010 (1960)	3180 (2110)	2990 (1930)	.89
Postoperative 48 wk	4240 (2200)	4450 (2520)	4150 (1810)	.87
Radiographic assessment of stem osseointegration (SD)				
Stability score at 2 y	8.4 (1.5)	8.0 (1.5)	8.5 (1.4)	.23
Fixation score at 2 y	8.5 (3.1)	8.6 (3.0)	8.3 (3.2)	.79

PROMs, patient-reported outcome measures; WOMAC, Western Ontario and McMaster Universities Osteoarthritis Index; SD, standard deviation; HHS, Harris hip score.
[a] Comparison of subjects with the radius cortical-bone thickness of ≥2.3 mm or <2.3 mm with 2-tailed Student *t*-test or chi-square test.

structural changes are typical in the proximal femur of postmenopausal women [18] and provide an obvious explanation for stem subsidence. In a retrospective evaluation, our eligibility criteria followed the recommendation [7] to use the parallel-sided femoral stem only in subjects with adequate bone stock (only 2 of our enrolled subjects had osteoporosis) and unaltered femoral geometry (we excluded subjects with Dorr type C femurs) rather closely. Stem subsidence appears to be a consequence of rather subtle geometric changes of the proximal femur, including Dorr type B deformity, but it is likely that structural alterations, such as endosteal trabeculation of the cortical bone [2], are more severe than appreciable on plain radiographs.

Although it has never been proven, the initial micromotion of a weight-bearing implant may affect the speed of recovery postoperatively. However, the clinical significance of the minor difference in subsidence (1.11 mm), found between the 2 groups, was questionable. The 2 groups were found to have no statistical differences in clinical recovery and radiographic osseointegration. Thus, further RSA studies are required to compare the speed of recovery in patients with high femoral component stability to that in patients who experience different degrees of initial stem subsidence.

As a study limitation, the limited group size and the inclusion of only postmenopausal women preclude implementation of the results to different groups of THA patients and different stem designs. Concerning the selection of the stem subsidence threshold, the limit of clinically significant migration remains incompletely defined for uncemented femoral stems [27]. The generalizability of the observed cutoff values remains to be verified in larger populations of different stems. It is noteworthy that the ROC curve-driven cutoff value of the distal radius BMD did not exactly follow the normal categorization of subjects with normal (T-score ≥ -1.0) and low (T-score < -1.0) BMDs. The measurement of cortical-bone thickness is a challenge [28], and pulse-echo ultrasonometry gives only a rough estimate of cortical-bone thickness. Preoperative imaging of the proximal femur using high-resolution computed tomography techniques [29,30] could demonstrate the real status of the cortical bone in postmenopausal women and achieve higher predictive accuracy of stem subsidence.

Conclusion

The diagnostic accuracy of the cortical-bone thickness of the radius measured by pulse-echo ultrasonometry was moderate and similar to that of the distal radius BMD in discriminating between <2 mm and ≥2 mm femoral stem subsidence. An increased risk of stem subsidence was a characteristic of postmenopausal women with cortical-bone thinning and a reduced BMD in both the proximal femur and distal radius. Compared with the distal radius BMD measured by DXA, pulse-echo ultrasonometry has the advantage of being portable and potentially applicable for office-based screening of impaired bone quality. The generalizability of the measured cutoff values remains to be verified using different stem designs in larger populations of postmenopausal women.

Acknowledgments

The original investigator-initiated RCT was supported by Amgen Inc (ISS #20109714, 2014), the Academy of Finland (decision #288607, 2015), and Turku University Hospital (government-sponsored research grants #13705, 2014-2017). The manufacturer provided the ultrasound device without charge. The funding sources had no involvement in the collection, analysis and interpretation of data, in the writing of the report, and in the decision to submit the article for publication. The authors received no financial support for the research, authorship, and/or publication of this article and the authors declare no potential conflicts of interest with respect to the research, authorship, and/or publication of this article.

References

[1] Khanuja HS, Vakil JJ, Goddard MS, Mont MA. Cementless femoral fixation in total hip arthroplasty. J Bone Joint Surg Am 2011;93:500–9. https://doi.org/10.2106/JBJS.J.00774.

[2] Zebaze RM, Ghasem-Zadeh A, Bohte A, Iuliano-Burns S, Mirams M, Price RI, et al. Intracortical remodelling and porosity in the distal radius and post-mortem femurs of women: a cross-sectional study. Lancet 2010;375:1729–36. https://doi.org/10.1016/S0140-6736(10)60320-0.

[3] Aro HT, Alm JJ, Moritz N, Mäkinen TJ, Lankinen P. Low BMD affects initial stability and delays stem osseointegration in cementless total hip arthroplasty in women. Acta Orthop 2012;83:107–14. https://doi.org/10.3109/17453674.2012.678798.

[4] Aro E, Moritz N, Mattila K, Aro HT. A long-lasting bisphosphonate partially protects periprosthetic bone, but does not enhance initial stability of uncemented femoral stems: a randomized placebo-controlled trial of women undergoing total hip arthroplasty. J Biomech 2018;75:35–45. https://doi.org/10.1016/j.jbiomech.2018.04.041.

[5] Issa K, Pivec R, Wuestemann T, Tatevossian T, Nevelos J, Mont MA. Radiographic fit and fill analysis of a new second-generation proximally coated cementless stem compared to its predicate design. J Arthroplasty 2014;29:192–8. https://doi.org/10.1016/j.arth.2013.04.029.

[6] Faizan A, Wuestemann T, Nevelos J, Bastian AC, Collopy D. Development and verification of a cementless novel tapered wedge stem for total hip arthroplasty. J Arthroplasty 2015;30:235–40. https://doi.org/10.1016/j.arth.2014.09.023.
[7] Grayson C, Meneghini RM. Parallel-sided femoral stems. In: Lieberman JR, Berry DJ, editors. Adv. Reconstr. Hip 2. Rosemont, IL: American Academy of Orthopaedic Surgeons and The Hip Society; 2017. p. 119–25.
[8] Aro HT, Nazari-Farsani S, Vuopio M, Löyttyniemi E, Mattila K. Effect of denosumab on femoral periprosthetic BMD and early femoral stem subsidence in postmenopausal women undergoing cementless total hip arthroplasty. JBMR Plus 2019;3:e10217. https://doi.org/10.1002/jbm4.10217.
[9] Nevitt MC, Lane NE, Scott JC, Hochberg MC, Pressman AR, Genant HK, et al. Radiographic osteoarthritis of the hip and bone mineral density. The study of osteoporotic fractures research group. Arthritis Rheum 1995;38:907–16.
[10] Lingard EA, Mitchell SY, Francis RM, Rawlings D, Peaston R, Birrell FN, et al. The prevalence of osteoporosis in patients with severe hip and knee osteoarthritis awaiting joint arthroplasty. Age Ageing 2010;39:234–9. https://doi.org/10.1093/ageing/afp222.
[11] Schousboe JT, Riekkinen O, Karjalainen J. Prediction of hip osteoporosis by DXA using a novel pulse-echo ultrasound device. Osteoporos Int 2017;28:85–93. https://doi.org/10.1007/s00198-016-3722-4.
[12] Karjalainen JP, Riekkinen O, Kröger H. Pulse-echo ultrasound method for detection of post-menopausal women with osteoporotic BMD. Osteoporos Int 2018;29:1193–9. https://doi.org/10.1007/s00198-018-4408-x.
[13] Zebaze R, Libanati C, McClung MR, Zanchetta JR, Kendler DL, Høiseth A, et al. Denosumab reduces cortical porosity of the proximal femoral shaft in postmenopausal women with osteoporosis. J Bone Miner Res 2016;31:1827–34. https://doi.org/10.1002/jbmr.2855.
[14] Grant TW, Lovro LR, Licini DJ, Warth LC, Ziemba-Davis M, Meneghini RM. Cementless tapered wedge femoral stems decrease subsidence in obese patients compared to traditional fit-and-fill stems. J Arthroplasty 2017;32:891–7. https://doi.org/10.1016/j.arth.2016.09.023.
[15] Nazari-Farsani S, Finnilä S, Moritz N, Mattila K, Alm JJ, Aro HT. Is model-based radiostereometric analysis suitable for clinical trials of a cementless tapered wedge femoral stem? Clin Orthop Relat Res 2016;474:2246–53. https://doi.org/10.1007/s11999-016-4930-0.
[16] Valstar ER, Gill R, Ryd L, Flivik G, Börlin N, Kärrholm J. Guidelines for standardization of radiostereometry (RSA) of implants. Acta Orthop 2005;76:563–72. https://doi.org/10.1080/17453670510041574.
[17] Derbyshire B, Prescott RJ, Porter ML. Notes on the use and interpretation of radiostereometric analysis. Acta Orthop 2009;80:124–30. https://doi.org/10.1080/17453670902807474.
[18] Noble PC, Box GG, Kamaric E, Fink MJ, Alexander JW, Tullos HS. The effect of aging on the shape of the proximal femur. Clin Orthop Relat Res 1995;316:31–44. https://doi.org/10.1097/00003086-199507000-00006.
[19] Engh CA, Massin P, Suthers KE. Roentgenographic assessment of the biologic fixation of porous-surfaced femoral components. Clin Orthop Relat Res 1990;257:107–28. https://doi.org/10.1097/00003086-199008000-00022.
[20] Foucher KC. Identifying clinically meaningful benchmarks for gait improvement after total hip arthroplasty. J Orthop Res 2016;34:88–96. https://doi.org/10.1002/jor.22996.
[21] Schwesig R, Leuchte S, Fischer D, Ullmann R, Kluttig A. Inertial sensor based reference gait data for healthy subjects. Gait Posture 2011;33:673–8. https://doi.org/10.1016/j.gaitpost.2011.02.023.
[22] Schmalzried TP, Szuszczewicz ES, Northfield MR, Akizuki KH, Frankel RE, Belcher G, et al. Quantitative assessment of walking activity after total hip or knee replacement. J Bone Joint Surg Am 1998;80:54–9.
[23] Campbell D, Mercer G, Nilsson KG, Wells V, Field JR, Callary SA. Early migration characteristics of a hydroxyapatite-coated femoral stem: an RSA study. Int Orthop 2011;35:483–8. https://doi.org/10.1007/s00264-009-0913-z.
[24] Sköldenberg OG, Salemyr MO, Bodén HS, Ahl TE, Adolphson PY. The effect of weekly risedronate on periprosthetic bone resorption following total hip arthroplasty: a randomized, double-blind, placebo-controlled trial. J Bone Joint Surg Am 2011;93:1857–64. https://doi.org/10.2106/JBJS.J.01646.
[25] Ström H, Nilsson O, Milbrink J, Mallmin H, Larsson S. The effect of early weight bearing on migration pattern of the uncemented CLS stem in total hip arthroplasty. J Arthroplasty 2007;22:1122–9. https://doi.org/10.1016/j.arth.2006.11.015.
[26] Dorr LD, Faugere MC, Mackel AM, Gruen TA, Bognar B, Malluche HH. Structural and cellular assessment of bone quality of proximal femur. Bone 1993;14:231–42. https://doi.org/10.1016/8756-3282(93)90146-2.
[27] van der Voort P, Pijls BG, Nieuwenhuijse MJ, Jasper J, Fiocco M, Plevier JWM, et al. Early subsidence of shape-closed hip arthroplasty stems is associated with late revision. Acta Orthop 2015;86:575–85. https://doi.org/10.3109/17453674.2015.1043832.
[28] Zebaze R, Seeman E. Cortical bone: a challenging geography. J Bone Miner Res 2015;30:24–9. https://doi.org/10.1002/jbmr.2419.
[29] Genant HK, Libanati C, Engelke K, Zanchetta JR, Høiseth A, Yuen CK, et al. Improvements in hip trabecular, subcortical, and cortical density and mass in postmenopausal women with osteoporosis treated with denosumab. Bone 2013;56:482–8. https://doi.org/10.1016/j.bone.2013.07.011.
[30] Zebaze R, Ghasem-Zadeh A, Mbala A, Seeman E. A new method of segmentation of compact-appearing, transitional and trabecular compartments and quantification of cortical porosity from high resolution peripheral quantitative computed tomographic images. Bone 2013;54:8–20. https://doi.org/10.1016/j.bone.2013.01.007.

Appendix

Supplementary Table 1
Comparison of Radiostereometric Analysis Migration of the Parallel-Sided Femoral Stem in Patients With Cortical-Bone Thickness of the Radius Above or Below the Cutoff Value.

	Radius Cortical-Bone Thickness		Mean Difference	95% CI	*P* Value
	≥2.33 mm Mean (SD) (N = 26)	<2.33 mm Mean (SD) (N = 27)			
Translation (mm)					
x-axis	0.15 (0.39)	−0.03 (0.45)	−0.18	−0.41 to 0.06	.13
y-axis	−1.31 (1.30)	−2.43 (1.51)	−1.11	−1.89 to −0.34	.006
z-axis	−0.21 (1.00)	−0.56 (0.85)	−0.35	−0.87 to 0.17	.19
Rotation (°)					
x-axis	−0.16 (1.21)	−0.59 (0.71)	−0.43	−0.98 to 0.13	.13
y-axis	0.69 (2.01)	0.54 (2.76)	−0.14	−1.49 to 1.21	.84
z-axis	0.29 (1.03)	0.18 (0.71)	−0.11	−0.61 to 0.38	.64

SD, standard deviation; CI, confidence interval.